Hindawi
Geofluids
Volume 2019, Article ID 6803512, 12 pages
https://doi.org/10.1155/2019/6803512

Research Article

Dynamic Shear Strength of Rock Joints and Its Influence on Key Blocks

Shuhong Wang[1], **Feili Wang**[1,2] **and Zhanguo Xiu**[1]

[1]*School of Resource and Civil Engineering, Northeastern University, Shenyang 110819, China*
[2]*Department of Civil & Mineral Engineering, University of Toronto, Toronto, Ontario, Canada M5S 1A4*

Correspondence should be addressed to Feili Wang; feili.wang@mail.utoronto.ca and Zhanguo Xiu; xiuzhanguo109@126.com

Received 29 May 2019; Revised 16 September 2019; Accepted 1 October 2019; Published 12 November 2019

Academic Editor: Umberta Tinivella

Shear strength deterioration of rock joints and its induced instability of key blocks subjected to dynamic disturbance constitute the mechanism of many geological disasters such as rockburst, landslide, and rockfall. In this study, the influence of dynamic disturbance on rock joints was quantified in the form of stress, of which model was established by quasistatic method. The dynamic shear strength of rock joints was analyzed theoretically following the Coulomb-Navier criterion and further investigated experimentally by split Hopkinson pressure bar (SHPB) tests with impact velocities of 4.850 m/s, 8.722 m/s, 12.784 m/s, and 16.935 m/s. The effect of engineering disturbance on shear strength of rock joints was measured, and a degradation coefficient was used to describe it quantitatively. Considering the degradation of dynamic shear strength of rock joints and its influence on block stability, the method for determining key blocks under dynamic disturbance was given. Implementing this method into the program of Geotechnical Structure and Model Analysis-3D (GeoSMA-3D) developed by the authors' team, the visualization of key blocks was achieved. From theoretical analysis and experimental investigation, it was figured out that the shear strength of rock joints is degraded under dynamic disturbance. The degradation of friction angle becomes more sensitive than that of cohesion. Additionally, numerical results show that the number of key blocks was increased with the increasing impact velocities.

1. Introduction

An appropriate evaluation of shear behavior of rock joints is vital, for instance, when analyzing the stability of rock slopes, designing excavations in jointed rock, and designing rock-socked piles [1]. A considerable amount of work has been conducted to describe the shear behavior of rock joints [2–8]. However, in a variety of geomechanical engineering applications, such as rock quarrying, rock drilling, rock excavation, and rock blasting, rock joints may be stressed and failed dynamically [9]. Many studies have indicated that the large-scale engineering work destroyed the original stress balance of rock joints and influenced their shear behavior. The collapse, landslides, and many other geological disasters may occur under engineering disturbance. That is to say the strength deterioration of rock joints bears significant advent impacts to the geotechnical disasters [10]. Studying the failure process and degradation characteristics of rock joints under dynamic loading is critical for analyzing the failure mechanism of unstable work under dynamic disturbance. In practice, not only the failure mechanism but the secure method used in the unstable engineering work should be studied. Many publications have shown that the instability of rock engineering is often manifested in the form of the slip of the blocks formed by the intersection of joints [11–15]. The methods used to judge the block stability and determine the key blocks show that block stability is dominated by shear behavior of rock joints. Obviously, the strength deterioration of rock joints inevitably induced the emergence of key blocks. Therefore, it is of great importance to judge the block stability and establish a method to determine the key blocks under engineering disturbance.

At shallow depth, jointed rock mass failure commonly occurs along weak discontinuities in shear mode [3]. An

appropriate evaluation of shear behavior of rock joints is vital. In conventional studies, the shear response of a joint was usually investigated in an experimental method or a theoretical way. With regard to shear behavior evaluation through laboratory investigation, the direct shear test and cyclic shear test have gained significant attention. Considering the spatial geometry and stress state of rock joints, direct shear tests [6, 16–20] and cyclic shear tests [7, 8, 21–25] were conducted by different researchers from around the world. It should, however, be noted that the aforementioned shear test requires a costly shear test apparatus, and moreover, it involves a difficult, complex, and time-consuming procedure of sample collection and preparation. Therefore, the estimation of shear strength empirically by using existing shear strength criteria has got obvious advantages. In the past few decades, many researchers proposed empirical shear strength criteria of joints considering their physical and geometrical characteristics [3, 26–32]. It should be noted that fruitful results have been achieved by different researchers from around the world on a regular basis which certainly have got significant academic importance. However, few existing publications regarding the dynamic shear behavior of rock joints were carried out. The dynamic shear strength of rock joints has a significant influence on the stability of rock engineering. With the increase of dynamic engineering activities, the research on dynamic shear strength of rock joints is urgently needed.

With the shear strength degradation of joints under engineering disturbance, the block stability will be influenced accordingly. Over the years, many methods have been put forward to estimate the block stability and determine the key blocks [33–36]. The existing investigation mainly analyzed the effects of joint morphology on key blocks [37–39], such as the rock bridge and the distribution or the length of joints. However, the shear strength of rock joints has been generally regarded as the most critical factor of the block stability, which is closely related to the safety factor of key blocks. Notably, in conventional studies, the key blocks determined by block theory were under static loading. However, in a variety of geological disasters, such as rockburst, landslide, and rockfall, the rock block may be stressed and failed dynamically. The accurate determination of key blocks under dynamic loading is thus desirable in many rock engineering applications, the shear strength should be considered at the same time.

With the limitation of test conditions and the difficulties in dynamic experimental investigation, the study on the dynamic properties of rock joints experiences a huge challenge, especially its shear behavior. Limited research on the dynamic shear behavior of rock mass was conducted. For example, a testing method called the punch-through shear test was introduced by Backers et al. [40, 41]; a series of laboratory tests on limestone, marble, and granite were presented, and the influence of confining pressure, loading rate, sample size, and cyclic loading was studied. Huang et al. [42] gave a dynamic punch method to quantify the dynamic shear strength of sandstone by a split Hopkinson pressure bar system (SHPB) with a specially designed holder. The punch-through shear (PTS) method was further studied by Yao et al. [9]; the dynamic Mode II fracture toughness of rocks was determined, and the dynamic fracture pattern and modes of the rock were analyzed. However, the exiting publications mainly focused on the shear behavior of rock mass not rock joints. For this, attempts are made to study the dynamic shear strength of rock joints in quasistatic method in this paper.

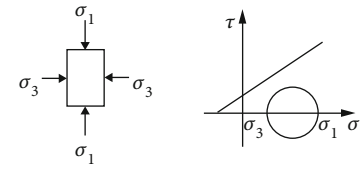

Figure 1: The stress state under self-weight.

In the present study, a stress model was established to evaluate the mechanical characteristics of rock joints under dynamic disturbance. The theoretical expression on the variation of joint shear strength was deduced by the established stress model and the Coulomb-Navier criterion. The detrimental effect of dynamic disturbance on the shear strength of rock joints was analyzed, and a degradation coefficient was used to describe it quantitatively. Considering the influence of joint shear strength on key blocks, a method for judging block stability under engineering disturbance was established. Moreover, the judgment method of block stability was implemented into the GeoSMA-3D software, which realized the visual analysis of block stability under dynamic disturbance.

2. Characterization on the Variation of Dynamic Shear Strength

The influence of dynamic disturbance on rock joints was quantified in the form of stress. The stress model was established. Combining the stress model and Coulomb-Navier criterion, the theoretical expression on the variation of joints shear strength under dynamic disturbance was determined.

2.1. Analysis on the Stress State. The stress state of rock joints under engineering disturbance was interpreted by the superposition of original stress state and engineering disturbance stress state [43]. In this study, the self-weight stress is considered as the original stress state, as shown in Figure 1.

Figure 1 indicates that the geostatic stresses have fixed orientation on each joint, while the engineering disturbance is a dynamic loading and its orientation should be considered in the stress state [44]. As the dynamic loading affect the joint shear in arbitrary direction, eight cases are considered in this study. The stress caused by engineering disturbance is applied to rock joints in the form of horizontal and vertical stress, and the original self-weight stress was considered at the same time. The orientations between the principal stresses of dynamic loading and the geostatic stress are shown in Figure 2.

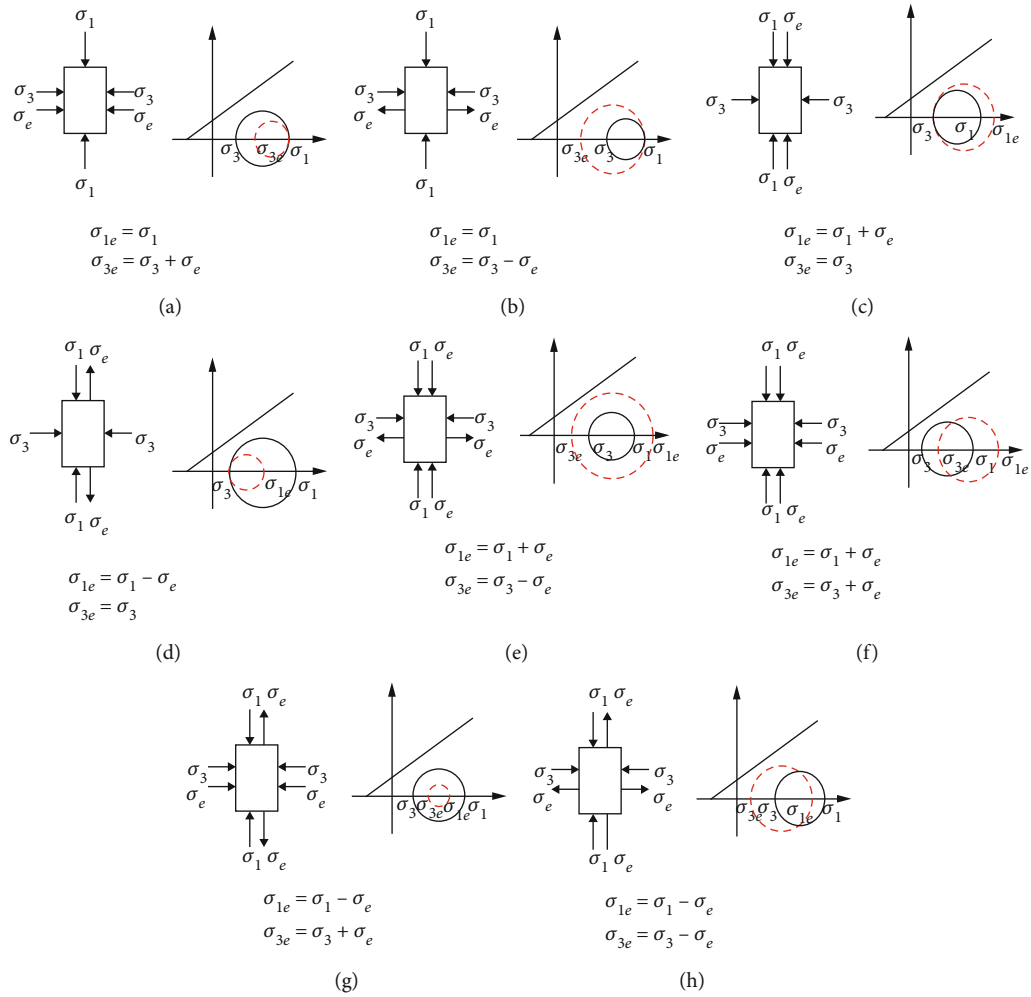

Figure 2: Stress state of rock joints under engineering disturbance.

It can be observed from Figures 2(b), 2(c), 2(e), 2(f), and 2(h) that the external dynamic loading can make the Mohr circle closer to the Coulomb-Navier failure envelope. In the practical analysis, the whole eight cases are checked out for failure on each joint and the one most unfavorable to joint properties is regarded as the final stress state.

Based on the analysis of stress state and the calculation of σ_{1e}, σ_{3e}, the formula of normal stress σ and shear stress τ under various stress states can be determined by stress equations on the shear plane.

$$\begin{aligned} \sigma &= \frac{\sigma_1 + \sigma_3}{2} + \frac{\sigma_1 - \sigma_3}{2} \cos 2\phi, \\ \tau &= \frac{\sigma_1 - \sigma_3}{2} \sin 2\phi, \end{aligned} \tag{1}$$

where σ_1, σ_3 is the maximum and minimum principal stress, respectively, ϕ is the angle between shear plane and the direction of the maximum principal stress.

In this study, the orientation of the principal stresses of dynamic loading on a joint is considered in eight forms which is reflected by the parameters k_1 and k_2 in equation (2). Its relationship with the principal geostatic stress under each stress state is shown in Table 1. The establishment and analysis of the stress model of rock joints under dynamic disturbance are realized.

$$\begin{aligned} \sigma &= \frac{\sigma_1 + \sigma_3 + (k_1 + k_2)\sigma_e}{2} + \frac{\sigma_1 - \sigma_3 + (k_1 - k_2)\sigma_e}{2} \cos 2\phi, \\ \tau &= \frac{\sigma_1 - \sigma_3 + (k_1 - k_2)\sigma_e}{2} \sin 2\phi \quad (k_1, k_2 = -1, 0, 1), \end{aligned} \tag{2}$$

where σ_e is the disturbance stress.

2.2. Theoretical Expression. Based on the stress model established above, the shear strength of rock joints was characterized. The effect of dynamic disturbance on the shear strength of rock joints was analyzed by the Coulomb-Navier criterion. Then, the theoretical expression on the degradation of dynamic shear strength can be obtained.

The Coulomb-Navier criterion considers that the shear failure along one side of rock joints is controlled not only by shear stress but also by normal stress [45]. The failure of

Table 1: The stress expression of rock joints.

Stress state	The formula of σ and τ
(*a*)	$\sigma = \frac{\sigma_1+\sigma_3+\sigma_e}{2} + \frac{\sigma_1-\sigma_3-\sigma_e}{2}\cos 2\phi$, $\tau = \frac{\sigma_1-\sigma_3-\sigma_e}{2}\sin 2\phi$
(*b*)	$\sigma = \frac{\sigma_1+\sigma_3-\sigma_e}{2} + \frac{\sigma_1-\sigma_3+\sigma_e}{2}\cos 2\phi$, $\tau = \frac{\sigma_1-\sigma_3+\sigma_e}{2}\sin 2\phi$
(*c*)	$\sigma = \frac{\sigma_1+\sigma_3+\sigma_e}{2} + \frac{\sigma_1+\sigma_e-\sigma_3}{2}\cos 2\phi$, $\tau = \frac{\sigma_1+\sigma_e-\sigma_3}{2}\sin 2\phi$
(*d*)	$\sigma = \frac{\sigma_1-\sigma_e+\sigma_3}{2} + \frac{\sigma_1-\sigma_e-\sigma_3}{2}\cos 2\phi$, $\tau = \frac{\sigma_1-\sigma_e-\sigma_3}{2}\sin 2\phi$
(*e*)	$\sigma = \frac{\sigma_1+\sigma_3}{2} + \frac{\sigma_1-\sigma_3+2\sigma_e}{2}\cos 2\phi$, $\tau = \frac{\sigma_1-\sigma_3+2\sigma_e}{2}\sin 2\phi$
(*f*)	$\sigma = \frac{\sigma_1+\sigma_3+2\sigma_e}{2} + \frac{\sigma_1-\sigma_3}{2}\cos 2\phi$, $\tau = \frac{\sigma_1-\sigma_3}{2}\sin 2\phi$
(*g*)	$\sigma = \frac{\sigma_1+\sigma_3}{2} + \frac{\sigma_1-\sigma_3-2\sigma_e}{2}\cos 2\phi$, $\tau = \frac{\sigma_1-\sigma_3-2\sigma_e}{2}\sin 2\phi$
(*h*)	$\sigma = \frac{\sigma_1+\sigma_3-2\sigma_e}{2} + \frac{\sigma_1-\sigma_3}{2}\cos 2\phi$, $\tau = \frac{\sigma_1-\sigma_3}{2}\sin 2\phi$

rock joints does not occur along the plane with maximum shear stress but ruptures along one of the faces where shear stress and normal stress reach the most unfavorable combination. The Coulomb-Navier criterion of rock joints can be expressed by

$$|\tau_f| = \tau_0 + f\sigma_n, \tag{3}$$

where $|\tau_f|$ is the shear strength of the shear plane, τ_0 is the inherent shear strength of rock joints which is similar to the definition of cohesion c, $f\sigma_n$ is the frictional resistance on the shear surface, σ_n is the normal stress on the shear plane, and $f = \tan\varphi$ is the friction coefficient of rock joints.

Table 2: The strength analysis criterion of rock joints.

Stress state	The strength analysis model
(*a*)	$2c = (\sigma_1-\sigma_3-\sigma_e)\sec\varphi - (\sigma_1+\sigma_3+\sigma_e)\tan\varphi$
(*b*)	$2c = (\sigma_1-\sigma_3+\sigma_e)\sec\varphi - (\sigma_1+\sigma_3-\sigma_e)\tan\varphi$
(*c*)	$2c = (\sigma_1+\sigma_e-\sigma_3)\sec\varphi - (\sigma_1+\sigma_e+\sigma_3)\tan\varphi$
(*d*)	$2c = (\sigma_1-\sigma_e-\sigma_3)\sec\varphi - (\sigma_1-\sigma_e+\sigma_3)\tan\varphi$
(*e*)	$2c = (\sigma_1-\sigma_3+2\sigma_e)\sec\varphi - (\sigma_1+\sigma_3)\tan\varphi$
(*f*)	$2c = (\sigma_1-\sigma_3)\sec\varphi - (\sigma_1+\sigma_3+2\sigma_e)\tan\varphi$
(*g*)	$2c = (\sigma_1-\sigma_3-2\sigma_e)\sec\varphi - (\sigma_1+\sigma_3)\tan\varphi$
(*h*)	$2c = (\sigma_1-\sigma_3)\sec\varphi - (\sigma_1+\sigma_3-2\sigma_e)\tan\varphi$

Equation (4) is the Coulomb-Navier criterion that is expressed by σ_1 and σ_3. If the stress state meets this formula, the rock joints will experience shear fracture.

$$2c = \sigma_1(\sec\varphi - \tan\varphi) - \sigma_3(\sec\varphi + \tan\varphi). \tag{4}$$

Considering the dynamic disturbance, σ_1, σ_3 are replaced by σ_{1e}, σ_{3e}. A strength analysis model corresponding to the stress state in Figure 2 was established, as shown in Table 2. The general form is given, as shown in

$$\begin{aligned} 2c = {} & [\sigma_1 - \sigma_3 + (k_1 - k_2)\sigma_e]\sec\varphi \\ & - [\sigma_1 + \sigma_3 + (k_1 + k_2)\sigma_e]\tan\varphi \quad (k_1, k_2 = -1, 0, 1). \end{aligned} \tag{5}$$

Based on the strength analysis criterion, the effect of dynamic disturbance on the shear strength of rock joints was analyzed by contrasting the shear strength parameters, c, φ, of rock joints under the original stress with c_e, φ_e of rock joints under dynamic disturbance. The degradation coefficients k_c, k_φ are used to describe the shear strength variation quantitatively, as shown in Table 3. The general form is given, as shown in

$$\begin{aligned} k_c &= \frac{c}{c_e} = \frac{(\sigma_1-\sigma_3) - (\sigma_1+\sigma_3)\sin\varphi}{[\sigma_1-\sigma_3+(k_1-k_2)\sigma_e]\sec\varphi - [\sigma_1+\sigma_3+(k_1+k_2)\sigma_e]\tan\varphi}, \\ k_\varphi &= \frac{\tan\varphi}{\tan\varphi_e} = \frac{\left[(\sigma_1-\sigma_3)\sqrt{c^2+\sigma_1\sigma_3} - c(\sigma_1+\sigma_3)\right][(\sigma_1+k_1\sigma_e)(\sigma_3+k_2\sigma_e)]}{\left\{[\sigma_1-\sigma_3+(k_1-k_2)\sigma_e]\sqrt{c^2+(\sigma_1+k_1\sigma_e)(\sigma_3+k_2\sigma_e)} - c[\sigma_1+\sigma_3+(k_1+k_2)\sigma_e]\right\}\sigma_1\sigma_3}. \end{aligned} \tag{6}$$

This process provides a theoretical method for analyzing the variation of joint shear strength under dynamic disturbance. A new idea for analyzing the induced mechanism of unstable works under engineering disturbance is given.

Table 3: The formula of k_c, k_φ for rock joints under engineering disturbance.

Stress state	The formula of k_c, k_φ
(*a*)	$k_c = \frac{c}{c_e} = \frac{(\sigma_1-\sigma_3)-(\sigma_1+\sigma_3)\sin\varphi}{(\sigma_1-\sigma_3-\sigma_e)-(\sigma_1+\sigma_3+\sigma_e)\sin\varphi} k_\varphi = \frac{\tan\varphi}{\tan\varphi_e} = \frac{\left[(\sigma_1-\sigma_3)\sqrt{c^2+\sigma_1\sigma_3}-c(\sigma_1+\sigma_3)\right](\sigma_3+\sigma_e)}{\left[(\sigma_1-\sigma_3-\sigma_e)\sqrt{c^2+\sigma_1(\sigma_3+\sigma_e)}-c(\sigma_1+\sigma_3+\sigma_e)\right]\sigma_3}$
(*b*)	$k_c = \frac{c}{c_e} = \frac{(\sigma_1-\sigma_3)-(\sigma_1+\sigma_3)\sin\varphi}{(\sigma_1-\sigma_3+\sigma_e)-(\sigma_1+\sigma_3-\sigma_e)\sin\varphi} k_\varphi = \frac{\tan\varphi}{\tan\varphi_e} = \frac{\left[(\sigma_1-\sigma_3)\sqrt{c^2+\sigma_1\sigma_3}-c(\sigma_1+\sigma_3)\right](\sigma_3-\sigma_e)}{\left[(\sigma_1-\sigma_3+\sigma_e)\sqrt{c^2+\sigma_1(\sigma_3-\sigma_e)}-c(\sigma_1+\sigma_3-\sigma_e)\right]\sigma_3}$
(*c*)	$k_c = \frac{c}{c_e} = \frac{(\sigma_1-\sigma_3)-(\sigma_1+\sigma_3)\sin\varphi}{(\sigma_1-\sigma_3+\sigma_e)-(\sigma_1+\sigma_3+\sigma_e)\sin\varphi} k_\varphi = \frac{\tan\varphi}{\tan\varphi_e} = \frac{\left[(\sigma_1-\sigma_3)\sqrt{c^2+\sigma_1\sigma_3}-c(\sigma_1+\sigma_3)\right](\sigma_1+\sigma_e)}{\left[(\sigma_1+\sigma_e-\sigma_3)\sqrt{c^2+\sigma_3(\sigma_1+\sigma_e)}-c(\sigma_1+\sigma_e+\sigma_3)\right]\sigma_1}$
(*d*)	$k_c = \frac{c}{c_e} = \frac{(\sigma_1-\sigma_3)-(\sigma_1+\sigma_3)\sin\varphi}{(\sigma_1-\sigma_3-\sigma_e)-(\sigma_1+\sigma_3-\sigma_e)\sin\varphi} k_\varphi = \frac{\tan\varphi}{\tan\varphi_e} = \frac{\left[(\sigma_1-\sigma_3)\sqrt{c^2+\sigma_1\sigma_3}-c(\sigma_1+\sigma_3)\right](\sigma_1-\sigma_e)}{\left[(\sigma_1-\sigma_e-\sigma_3)\sqrt{c^2+\sigma_3(\sigma_1-\sigma_e)}-c(\sigma_1-\sigma_e+\sigma_3)\right]\sigma_1}$
(*e*)	$k_c = \frac{c}{c_e} = \frac{(\sigma_1-\sigma_3)-(\sigma_1+\sigma_3)\sin\varphi}{(\sigma_1-\sigma_3+2\sigma_e)-(\sigma_1+\sigma_3)\sin\varphi} k_\varphi = \frac{\tan\varphi}{\tan\varphi_e} = \frac{\left[(\sigma_1-\sigma_3)\sqrt{c^2+\sigma_1\sigma_3}-c(\sigma_1+\sigma_3)\right][(\sigma_1+\sigma_e)(\sigma_3-\sigma_e)]}{\left[(\sigma_1-\sigma_3+2\sigma_e)\sqrt{c^2+(\sigma_1+\sigma_e)(\sigma_3-\sigma_e)}-c(\sigma_1+\sigma_3)\right]\sigma_1\sigma_3}$
(*f*)	$k_c = \frac{c}{c_e} = \frac{(\sigma_1-\sigma_3)-(\sigma_1+\sigma_3)\sin\varphi}{(\sigma_1-\sigma_3)-(\sigma_1+\sigma_3+2\sigma_e)\sin\varphi} k_\varphi = \frac{\tan\varphi}{\tan\varphi_e} = \frac{\left[(\sigma_1-\sigma_3)\sqrt{c^2+\sigma_1\sigma_3}-c(\sigma_1+\sigma_3)\right][(\sigma_1+\sigma_e)(\sigma_3+\sigma_e)]}{\left[(\sigma_1-\sigma_3)\sqrt{c^2+(\sigma_1+\sigma_e)(\sigma_3+\sigma_e)}-c(\sigma_1+\sigma_3+2\sigma_e)\right]\sigma_1\sigma_3}$
(*g*)	$k_c = \frac{c}{c_e} = \frac{(\sigma_1-\sigma_3)-(\sigma_1+\sigma_3)\sin\varphi}{(\sigma_1-\sigma_3-2\sigma_e)-(\sigma_1+\sigma_3)\sin\varphi} k_\varphi = \frac{\tan\varphi}{\tan\varphi_e} = \frac{\left[(\sigma_1-\sigma_3)\sqrt{c^2+\sigma_1\sigma_3}-c(\sigma_1+\sigma_3)\right][(\sigma_1-\sigma_e)(\sigma_3+\sigma_e)]}{\left[(\sigma_1-\sigma_3-2\sigma_e)\sqrt{c^2+(\sigma_1-\sigma_e)(\sigma_3+\sigma_e)}-c(\sigma_1+\sigma_3)\right]\sigma_1\sigma_3}$
(*h*)	$k_c = \frac{c}{c_e} = \frac{(\sigma_1-\sigma_3)-(\sigma_1+\sigma_3)\sin\varphi}{(\sigma_1-\sigma_3)-(\sigma_1+\sigma_3-2\sigma_e)\sin\varphi} k_\varphi = \frac{\tan\varphi}{\tan\varphi_e} = \frac{\left[(\sigma_1-\sigma_3)\sqrt{c^2+\sigma_1\sigma_3}-c(\sigma_1+\sigma_3)\right][(\sigma_1-\sigma_e)(\sigma_3-\sigma_e)]}{\left[(\sigma_1-\sigma_3)\sqrt{c^2+(\sigma_1-\sigma_e)(\sigma_3-\sigma_e)}-c(\sigma_1+\sigma_3-2\sigma_e)\right]\sigma_1\sigma_3}$

3. Quantification of the Degradation Coefficients

The effect of engineering disturbance on the shear strength of rock joints was expressed theoretically. In this section, the variation of joint shear strength under dynamic disturbance will be analyzed quantitatively and the value of degradation coefficient will be given in experimental method by SHPB tests.

3.1. Methods. In this study, a 100 mm diameter SHPB system is utilized to exert the impact loading [46, 47]; its physical and mechanical properties are given in Table 4.

In our configuration, a loading stress pulse is induced by the impact of the striking system composed of a gas gun and a striker bar on the incident bar, as shown in Figure 3. Stresses are transmitted to the specimen via the incident bar, and we record the complete dynamic stressing history using strain gauges on the incident and transmitted bars equidistant from the specimen, each set consists of two gauges located diametrically opposite [47]. Based on the strains derived from these three waves in the elastic bars, the loading forces on the two ends of the specimen can be calculated.

Further, to ensure the accuracy of the measurement results with the simple one-wave analysis, one has to guarantee valid testing conditions with some testing techniques, e.g., stress equilibrium for sample, failure sequences of sample, slenderness ratio of sample, and proper lubrication for minimizing the friction effect [47]. In this study, a small piece of brass with 50 mm diameter and 1 mm thickness is selected as the pulse shaper which is adhered on the top surface of the incident bar to reach such dynamic force equilibrium. Lubricants were used on the interfaces between bar and specimen to minimize the radial inertial effect and achieve uniform deformation of the specimen.

In this test, the specimen containing fractures is composed of a cylinder of red sandstone filled with the sand. The diameter and length of each cylinder are 100 and 50 mm, respectively. The rectangular fracture with the dimensions of 50 × 40 × 4mm is paralleled to the longitudinal

Table 4: Physical and mechanical properties of SHPB.

Properties	Unit	Values
The diameter of input (output) bar	mm	100
The length of input (output) bar	mm	4000
Young's modulus	GPa	206
The density	kg/m^3	7850
The wave propagation velocity	m/s	5122.698

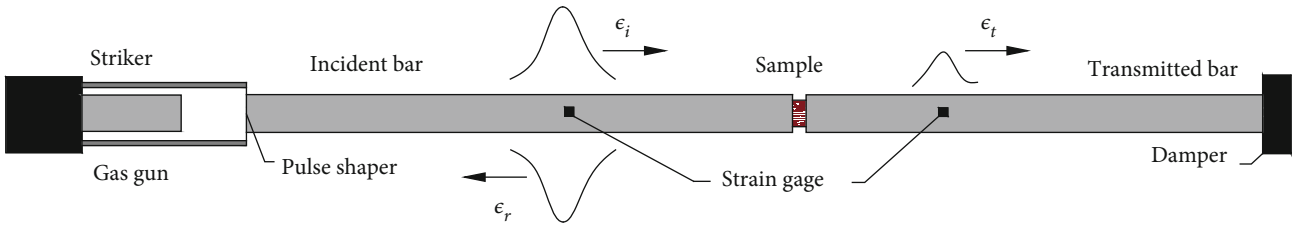

Figure 3: The SHPB apparatus.

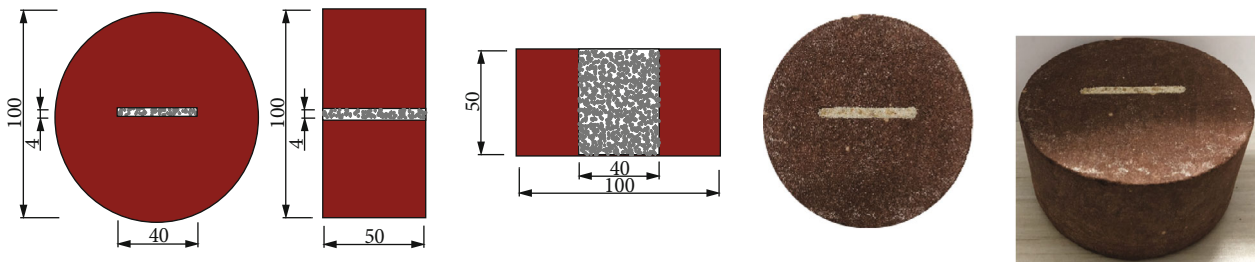

Figure 4: Schematics of the specimen.

axis of the cylindrical specimen. The schematics and pictures of the specimen were shown in Figure 4. The end surfaces shall not depart from perpendicularity to the longitudinal axis of the specimen by more than 0.5° and are flat to 0.01 mm. In addition, the surfaces of the specimen cylinder are smooth, free of abrupt irregularities, and straight to within 0.5 mm over the full length of the specimen since such irregularities might act as stress concentrators. Moreover, the deviation between the connecting line of the center points in both ends of the specimen and the specimen axis did not exceed 0.025 mm every 25 mm in length.

The specimens are divided into four groups according to the impact velocity, i.e., 4.850 m/s, 8.722 m/s, 12.784 m/s, and 16.935 m/s, respectively. With respect to different impact velocities, four test groups were conducted to investigate the effects of impact velocity on the strength degradation of rock structure. Each test group includes three tests to guarantee the repeatability of the experimental study.

In this test, pairs of diametrically oriented strain gauges are glued on the surfaces of the incident and transmitted bars. A digital oscilloscope connected to the gauges is applied to record and store the amplified strain signals collected from Wheatstone bridge circuits. The incident and reflected waves propagating in the input bar and the transmitted wave propagating in the output bar can be obtained from the records of strain gauges. The recorded strains from the test are used to determine the dynamic response in the specimen.

3.2. Results. The stress wave of the specimen with different impact velocities is given in Figure 5. Figure 5 indicated that the wave forms of the transmitted and reflected waves are very similar while impact velocities are different. But the amplitude of stress wave is different, which is associated with the impact velocity. It can be observed from Figure 5 that the amplitude of the transmitted wave decreases while the amplitude of the reflected wave increases with the increasing impact velocity.

The stress state of the sample subjected to impact loading with different velocities of 4.850 m/s, 8.722 m/s, 12.784 m/s, and 16.935 m/s is shown in Figure 6. It can be observed that the stress forms are similar while the impact velocity varies. The peak stresses increase with increasing impact velocity. The largest stresses acting on specimens were 58.38 MPa, 89.55 MPa, 95.23 MPa, and 106.3 MPa when the impact velocity was 4.850 m/s, 8.722 m/s, 12.784 m/s, and 16.935 m/s, respectively.

Combining the theoretical analysis in Section 2 with this experimental study, the relation between impact velocity and degradation coefficient can be obtained. The degradation coefficient of internal friction angle φ is 3.0524, 5.4119, 5.8386, and 6.669 for the impact velocity of 4.850 m/s, 8.722 m/s, 12.784 m/s, and 16.935 m/s, respectively. The corresponding degradation coefficient of cohesion c is 0.461, 0.292, 0.274, and 0.244. The effect of impact velocity on the degradation coefficient and the corresponding fitting curves are shown in Figure 7. The fitting curve results revealed that the tendency of k_φ rises with the increase of impact velocity. In comparison, it is also indicated that k_c decreases with the increase of impact velocity. This phenomenon suggests that the strength of jointed rock is degraded under impact loading. Additionally, the degradation of the internal friction angle becomes more obvious than that of cohesion.

4. Influence on Key Blocks

Based on the block theory and modern computer technique, a three-dimensional numerical software GeoSMA-3D is developed for identifying key blocks [15, 48, 49]. The main procedures include three dimension discontinuities network simulation, analysis of intersecting lines between discontinuities and surfaces, analysis of primary loops, loops location analysis, isolated loops deleting, relative loop analysis, closed block identification, and key block determination [48, 49].

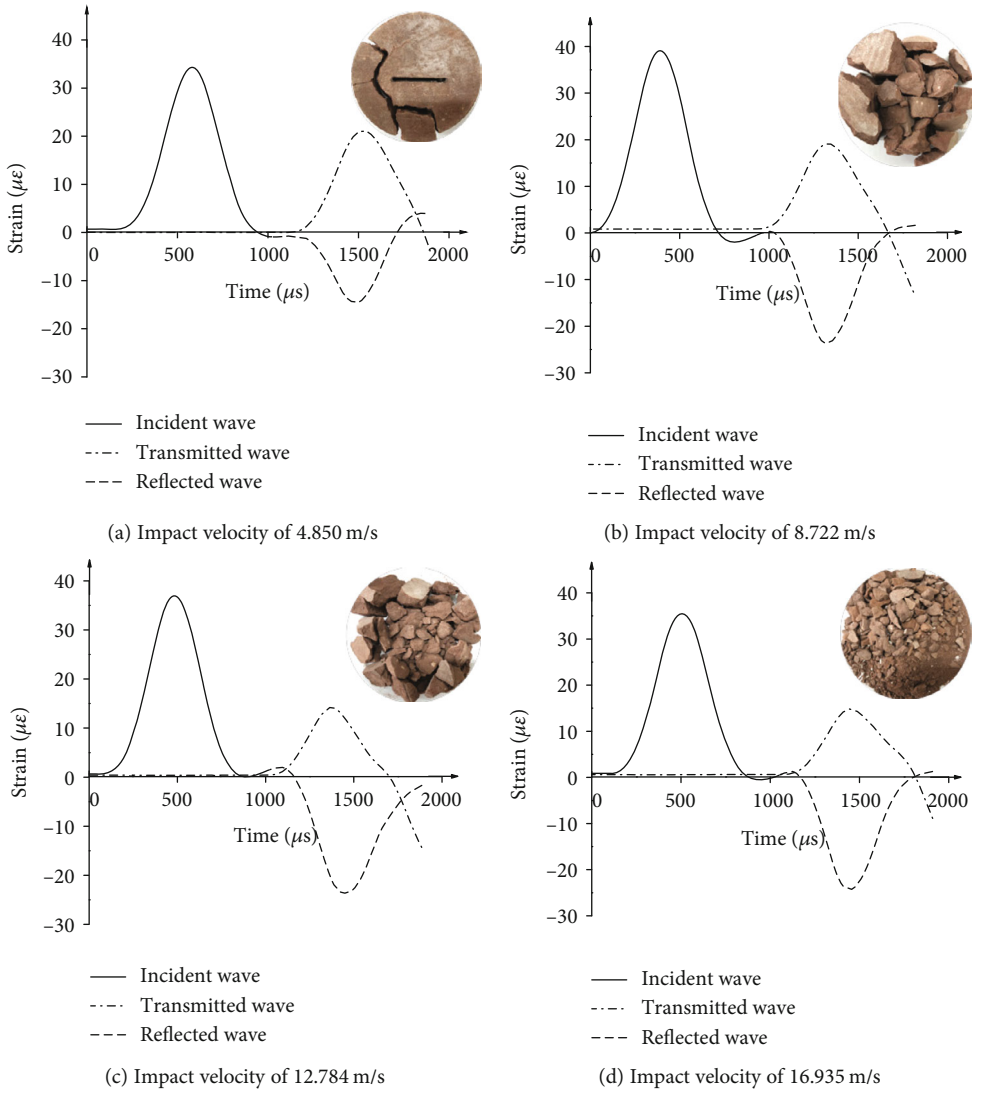

Figure 5: Stress wave of specimen with different impact velocity.

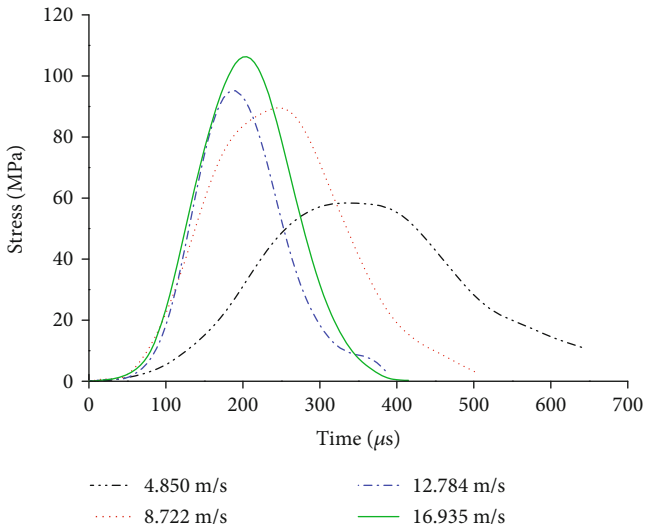

Figure 6: Curves of stress versus time with different impact velocities.

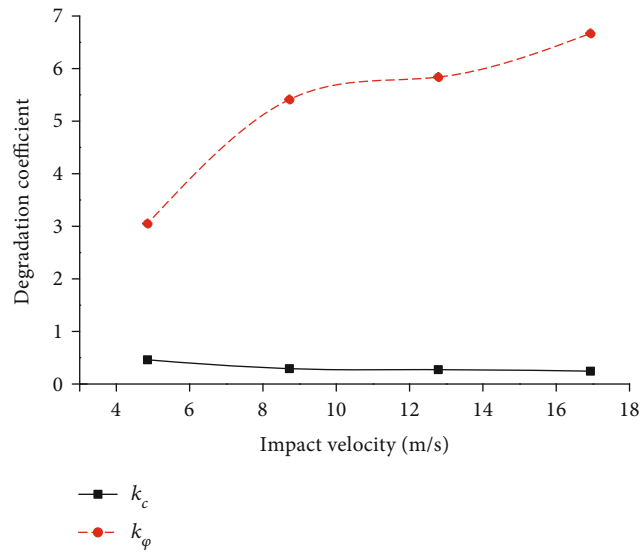

Figure 7: Curves of degradation coefficient versus impact velocities.

The block search module in GeoSMA-3D was used to determine the key blocks based on the classical block theory. In order to establish a key block judgment method which can realize the determination and visualization of key blocks under engineering disturbance, the formula for calculating the safety factors of block was modified by applying k_c and k_φ to reflect the deteriorating effect of shear strength on joints under engineering disturbance. The formula for judging block stability under engineering disturbance was given. With this method linked to the search module of key blocks in the program GeoSMA-3D, the determination and visualization of key blocks under engineering disturbance were achieved.

4.1. Determination of Key Blocks. The key blocks are determined by the safety factor based on block theory. From the formula of safety factor, we can see that the shear strength of rock joints influenced the value of safety factor strongly. Considering the degradation of dynamic shear strength of rock joints, the determination of key blocks under dynamic disturbance can be given.

4.1.1. The Block Is Separated from the Jointed Rock. If the movement of the block is in the form of falling, the safety factor is zero.

4.1.2. The Block Slides along a Single Surface. The sliding model for blocks which slides along a single surface is shown in Figure 8. Applying k_c and k_φ to reflect the effect of dynamic disturbance on the shear strength of rock joints, the stability of blocks under dynamic disturbance can be determined. In this sliding model, the safety factor η can be calculated by

$$\eta = \frac{G\cos\theta\tan\varphi_e + c_e S}{G\sin\theta}, \tag{7}$$

where

$$\tan\varphi_e = \frac{\tan\varphi}{k_\varphi}, c_e = \frac{c}{k_c}, \tag{8}$$

where G is the gravity of the block; S is the area of the sliding plane; θ is the dip angle of slipping plane; φ_e, c_e is the internal friction angle and cohesion of rock joints under engineering disturbance, respectively, and k_φ, k_c is the degradation coefficient of internal friction angle and cohesion, respectively.

4.1.3. The Block Slides along Bilateral Surfaces. The sliding model for blocks which slides along bilateral surfaces is shown in Figure 9. In this model, the safety factor η of the block can be calculated by

$$\eta = \frac{N_1\tan\varphi_{1e} + N_2\tan\varphi_{2e} + c_{1e}S_1 + c_{2e}S_2}{G\sin\theta}, \tag{9}$$

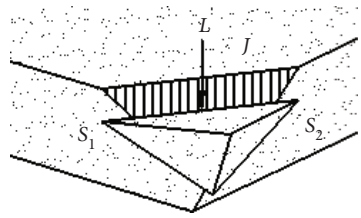

Figure 8: Model of single sliding surface.

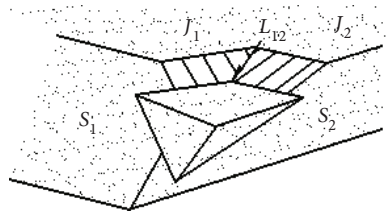

Figure 9: Model of bilateral sliding surfaces.

where

$$\tan\varphi_{1e} = \frac{\tan\varphi_1}{k_{1\varphi}}, \tan\varphi_{2e} = \frac{\tan\varphi_2}{k_{2\varphi}}, c_{1e} = \frac{c_1}{k_{1c}}, c_{2e} = \frac{c_2}{k_{2c}}, \tag{10}$$

where θ is the dip of the intersection of the slipping plane J_1 and J_2; N_1 and N_2 are the normal force of the slipping planes, φ_{1e}, c_{1e} and φ_{2e}, c_{2e} are the internal friction angle and cohesion of joints J_1 and J_2 under engineering disturbance, respectively, $k_{1\varphi}$, k_{1c} are the degradation coefficient of φ_{1e}, c_{1e}; and $k_{2\varphi}$, k_{2c} are the degradation coefficient of φ_{2e}, c_{2e}.

4.2. Visualization of Key Blocks. Combining the information of joints derived from ShapeMetriX3D with the block search module in the GeoSMA-3D software, the judgment of block stability and the visualization of key blocks can be achieved. The block search module in GeoSMA-3D can provide the visualization of key blocks, as well as quantitative information such as the safety factor, volume, and sliding surface of key blocks [15, 48, 49]. The key blocks determined in the original procedure were under static loading. In order to determine the key blocks under engineering disturbance, the judgment method should be improved.

Based on the calculation formula of the safety factor of the block, the stability judgment formula of the block under engineering disturbance is given by using the reduction coefficient of the damage effect under engineering disturbance. The judgment method of block stability is implemented into the GeoSMA-3D software. Combining with the original block search module in the system, the search and visual analysis of key blocks under engineering disturbance could be realized.

The strength degradation of rock joints varies with different levels of impact loading, resulting in different number and distribution of key blocks. Combining the degradation coefficient given in Section 3 and the safety factor realized

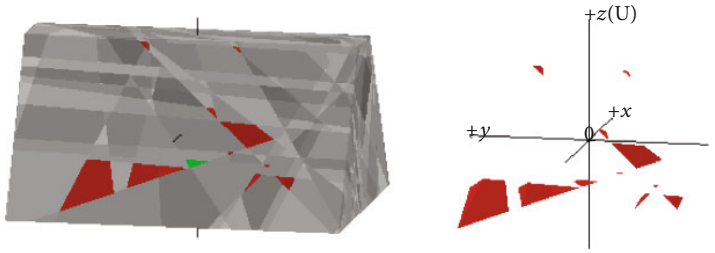

(a) The number and distribution of key blocks under static loading

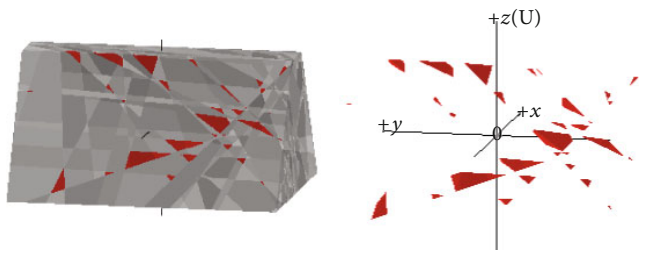

(b) The key blocks under the impact velocity of 4.850 m/s

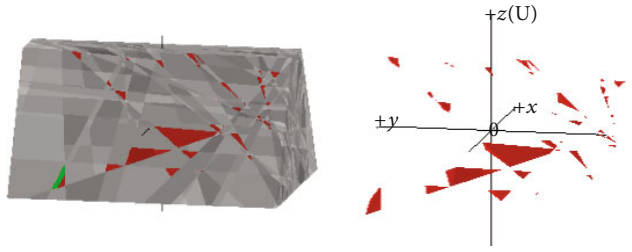

(c) The key blocks under the impact velocity of 8.722 m/s

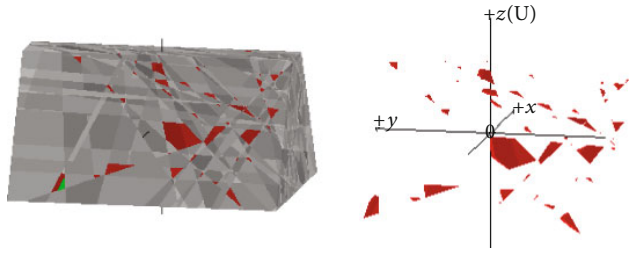

(d) The key blocks under the impact velocity of 12.784 m/s

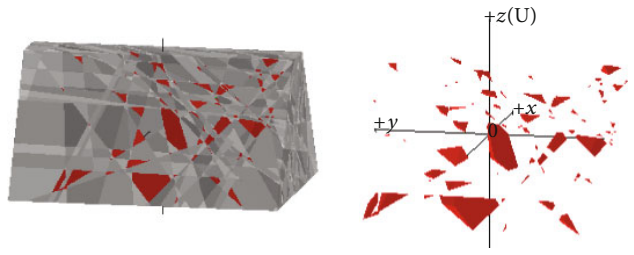

(e) The key blocks under the impact velocity of 16.935 m/s

Figure 10: The number and distribution of key blocks under different impact disturbances.

in Section 4, the key blocks can be determined under the impact velocity of 4.850 m/s, 8.722 m/s, 12.784 m/s, and 16.935 m/s, respectively. Figure 10(a) shows the key blocks under static loading, while Figures 10(b)–10(e) illustrate the key blocks under different impact loading, for example, 4.850 m/s, 8.722 m/s, 12.784 m/s, and 16.935 m/s, respectively. Figure 10 revealed that the number of key blocks becomes more with the increase of impact velocity.

Different impact velocities in the test and simulation represent different degrees of engineering disturbances on rock joints. After a series of theoretical study, experimental investigation, and numerical simulation, the dynamic shear

strength of rock joints was quantified and its influence on key blocks was determined.

5. Discussion

From the theoretical expression and experimental quantification on the variation of dynamic shear strength of rock joints, we can see that the degradation coefficient of the internal friction angle k_φ rises with the increase of impact velocities. In comparison, it is also indicated that the degradation coefficient of cohesion k_c decreases with the increasing impact velocities. And the degradation of internal friction angle φ becomes more sensitive than that of cohesion c. Notably, the value of k_φ is larger than one, while the value of k_c is smaller than one. That is to say, the internal friction angle of rock joints was degraded with the influence of dynamic disturbance, while the cohesion was upgraded. It is not difficult to understand that the dynamic impact has a negative effect on the internal friction angle of rock joints, but how to explain the positive effect on the cohesion. The tendency of k_c has shown that its value was decreased with the increasing impact velocities, which indicated that the value of c_e was increased with the increasing grade of disturbance. This phenomenon has shown that it is the dynamic cohesion provided by the high speed impact that caused the positive effect on the cohesion of rock joints.

From the method determined key blocks, we can see that the variation of joint shear strength affected the block stability strongly. The blocks formed by the intersection of joints with higher shear strength will be more stable. As the shear strength of joints was influenced by dynamic impact, the number and distribution of key blocks are related to the degree of engineering disturbances closely. The theoretical study and experimental investigation have shown that the internal friction angle φ was decreased while the cohesion was increased with the increasing impact velocities. But the degradation of internal friction angle φ becomes more sensitive than the upgradation of cohesion c, so their combining variation has a negative effect on the block stability. As shown in the numerical simulation, with the increase of impact velocity, more and more key blocks appeared.

6. Conclusion

In this study, the influence of engineering disturbance on rock joints was quantified in the form of stress and the stress model was established. The variation of joint shear strength under dynamic disturbance was quantified, and its influence on block stability was analyzed. The method on determination and visualization of key blocks under engineering disturbance was given. After a series of theoretical study, experimental investigation, and numerical simulation, some conclusions can be drawn as follows:

(1) The stress state related to different kinds of disturbance was analyzed. Using the quasistatic method, the stress model of rock joints under dynamic disturbance was analyzed. The shear strength criterion of rock joints under dynamic loading was established following the Coulomb-Navier criterion. Then, the theoretical expression on the variation of dynamic shear strength was given

(2) SHPB tests on the rock joints with different impact velocities of 4.850 m/s, 8.722 m/s, 12.784 m/s, and 16.935 m/s, respectively. The variation of joint shear strength under dynamic disturbance was quantified. The shear strength of rock joints was degraded under dynamic loading. The degradation of internal friction angle φ becomes more sensitive than that of cohesion c

(3) Considering the degradation of dynamic shear strength of rock joints, the method for judging block stability under dynamic disturbance was given. Implementing this method into GeoSMA-3D, the determination and visualization of key blocks under dynamic disturbance were achieved. The numerical simulation shows that the number and distribution of key blocks are related to the degree of engineering disturbances closely. With the increase of impact velocity, more and more key blocks appeared

Data Availability

All data, models, and code generated or used during the study appear in the submitted article.

Conflicts of Interest

The authors declare that there is no conflict of interest regarding the publication of this paper.

Acknowledgments

This work was conducted with supports from the National Natural Science Foundation of China (Grant Nos. 51474050 and U1602232), the Doctoral Scientific Research Foundation of Liaoning Province (Grant Nos. 20170540304 and 20170520341), the China Scholarship Council (Grant No. 201806080103), the Key Research and Development Program of Science and Technology in Liaoning Province, China (Grant No. 2019JH2/10100035), and the Fundamental Research Funds for the Central Universities (Grant No. N170108029).

References

[1] S. Thirukumaran and B. Indraratna, "A review of shear strength models for rock joints subjected to constant normal stiffness," *Journal of Rock Mechanics and Geotechnical Engineering*, vol. 8, no. 3, pp. 405–414, 2016.

[2] J. Cheng, H. Zhang, and Z. Wan, "Numerical simulation of shear behavior and permeability evolution of rock joints with variable roughness and infilling thickness," *Geofluids*, vol. 2018, Article ID 1869458, 11 pages, 2018.

[3] H. K. Singh and A. Basu, "Evaluation of existing criteria in estimating shear strength of natural rock discontinuities," *Engineering Geology*, vol. 232, pp. 171–181, 2018.

[4] R. Kumar and A. K. Verma, "Anisotropic shear behavior of rock joint replicas," *International Journal of Rock Mechanics and Mining Sciences*, vol. 90, pp. 62–73, 2016.

[5] Z. C. Tang, Y. Y. Jiao, L. N. Y. Wong, and X. C. Wang, "Choosing appropriate parameters for developing empirical shear strength criterion of rock joint: review and new insights," *Rock Mechanics and Rock Engineering*, vol. 49, no. 11, pp. 4479–4490, 2016.

[6] Y. K. Lee, J. W. Park, and J. J. Song, "Model for the shear behavior of rock joints under CNL and CNS conditions," *International Journal of Rock Mechanics and Mining Sciences*, vol. 70, pp. 252–263, 2014.

[7] A. Mirzaghorbanali, J. Nemcik, and N. Aziz, "Effects of shear rate on cyclic loading shear behaviour of rock joints under constant normal stiffness conditions," *Rock Mechanics and Rock Engineering*, vol. 47, no. 5, pp. 1931–1938, 2014.

[8] H. Atapour and M. Moosavi, "The influence of shearing velocity on shear behavior of artificial joints," *Rock Mechanics and Rock Engineering*, vol. 47, no. 5, pp. 1745–1761, 2014.

[9] W. Yao, Y. Xu, C. Yu, and K. Xia, "A dynamic punch-through shear method for determining dynamic Mode II fracture toughness of rocks," *Engineering Fracture Mechanics*, vol. 176, pp. 161–177, 2017.

[10] E. A. Chi, T. J. Tao, M. S. Zhao, and Q. Kang, "Failure mode analysis of bedding rock slope affected by rock mass structural plane," *Applied Mechanics and Materials*, vol. 602-605, pp. 594–597, 2014.

[11] Y. Zhang, M. Xiao, and J. Chen, "A new methodology for block identification and its application in a large scale underground cavern complex," *Tunnelling and Underground Space Technology*, vol. 25, no. 2, pp. 168–180, 2010.

[12] J. Zheng, P. H. S. W. Kulatilake, B. Shu, T. Sherizadeh, and J. Deng, "Probabilistic block theory analysis for a rock slope at an open pit mine in USA," *Computers and Geotechnics*, vol. 61, pp. 254–265, 2014.

[13] G. Sun, H. Zheng, and Y. Huang, "Stability analysis of statically indeterminate blocks in key block theory and application to rock slope in Jinping-I Hydropower Station," *Engineering Geology*, vol. 186, pp. 57–67, 2015.

[14] J. Zheng, P. H. S. W. Kulatilake, and J. Deng, "Development of a probabilistic block theory analysis procedure and its application to a rock slope at a hydropower station in China," *Engineering Geology*, vol. 188, pp. 110–125, 2015.

[15] F. Wang, S. Wang, M. Z. Hashmi, and Z. Xiu, "The characterization of rock slope stability using key blocks within the framework of GeoSMA-3D," *Bulletin of Engineering Geology and the Environment*, vol. 77, no. 4, pp. 1405–1420, 2018.

[16] B. K. Son, Y. K. Lee, and C. I. Lee, "Elasto-plastic simulation of a direct shear test on rough rock joints," *International Journal of Rock Mechanics and Mining Sciences*, vol. 41, pp. 354–359, 2004.

[17] S. Du, Y. Hu, X. Hu, and X. Guo, "Comparison between empirical estimation by JRC-JCS model and direct shear test for joint shear strength," *Journal of Earth Science*, vol. 22, no. 3, pp. 411–420, 2011.

[18] M. Sanei, L. Faramarzi, A. Fahimifar, S. Goli, A. Mehinrad, and A. Rahmati, "Shear strength of discontinuities in sedimentary rock masses based on direct shear tests," *International Journal of Rock Mechanics and Mining Sciences*, vol. 75, pp. 119–131, 2015.

[19] J. Yang, G. Rong, D. Hou, J. Peng, and C. Zhou, "Experimental study on peak shear strength criterion for rock joints," *Rock Mechanics and Rock Engineering*, vol. 49, no. 3, pp. 821–835, 2016.

[20] X. Zhang, Q. Jiang, N. Chen, W. Wei, and X. Feng, "Laboratory investigation on shear behavior of rock joints and a new peak shear strength criterion," *Rock Mechanics and Rock Engineering*, vol. 49, no. 9, pp. 3495–3512, 2016.

[21] A. M. Crawford and J. H. Curran, "The influence of shear velocity on the frictional resistance of rock discontinuities," *International Journal of Rock Mechanics and Mining Sciences & Geomechanics Abstracts*, vol. 18, no. 6, pp. 505–515, 1981.

[22] R. W. Hutson and C. H. Dowding, "Joint asperity degradation during cyclic shear," *International Journal of Rock Mechanics and Mining Sciences & Geomechanics Abstracts*, vol. 27, no. 2, pp. 109–119, 1990.

[23] L. Jing, O. Stephansson, and E. Nordlund, "Study of rock joints under cyclic loading conditions," *Rock Mechanics and Rock Engineering*, vol. 26, no. 3, pp. 215–232, 1993.

[24] H. S. Lee, Y. J. Park, T. F. Cho, and K. H. You, "Influence of asperity degradation on the mechanical behavior of rough rock joints under cyclic shear loading," *International Journal of Rock Mechanics and Mining Sciences*, vol. 38, no. 7, pp. 967–980, 2001.

[25] M. K. Jafari, K. A. Hosseini, F. Pellet, M. Boulon, and O. Buzzi, "Evaluation of shear strength of rock joints subjected to cyclic loading," *Soil Dynamics and Earthquake Engineering*, vol. 23, no. 7, pp. 619–630, 2003.

[26] N. Barton and V. Choubey, "The shear strength of rock joints in theory and practice," *Rock Mechanics*, vol. 10, no. 1-2, pp. 1–54, 1977.

[27] P. H. S. W. Kulatilake, G. Shou, T. H. Huang, and R. M. Morgan, "New peak shear strength criteria for anisotropic rock joints," *International Journal of Rock Mechanics and Mining Sciences & Geomechanics Abstracts*, vol. 32, no. 7, pp. 673–697, 1995.

[28] J. Zhao, "Joint surface matching and shear strength part B: JRC-JMC shear strength criterion," *International Journal of Rock Mechanics and Mining Sciences*, vol. 34, no. 2, pp. 179–185, 1997.

[29] G. Grasselli and P. Egger, "Constitutive law for the shear strength of rock joints based on three-dimensional surface parameters," *International Journal of Rock Mechanics and Mining Sciences*, vol. 40, no. 1, pp. 25–40, 2003.

[30] C. C. Xia, Z. C. Tang, W. M. Xiao, and Y. L. Song, "New peak shear strength criterion of rock joints based on quantified surface description," *Rock Mechanics and Rock Engineering*, vol. 47, no. 2, pp. 387–400, 2014.

[31] Z. C. Tang, Q. S. Liu, and J. H. Huang, "New criterion for rock joints based on three-dimensional roughness parameters," *Journal of Central South University*, vol. 21, no. 12, pp. 4653–4659, 2014.

[32] Z. C. Tang and L. N. Y. Wong, "New criterion for evaluating the peak shear strength of rock joints under different contact states," *Rock Mechanics and Rock Engineering*, vol. 49, no. 4, pp. 1191–1199, 2016.

[33] Q. Jiang, X. Liu, W. Wei, and C. Zhou, "A new method for analyzing the stability of rock wedges," *International Journal of Rock Mechanics and Mining Sciences*, vol. 60, pp. 413–422, 2013.

[34] Q. Jiang and C. Zhou, "A rigorous solution for the stability of polyhedral rock blocks," *Computers and Geotechnics*, vol. 90, pp. 190–201, 2017.

[35] M. Mauldon and J. Ureta, "Stability analysis of rock wedges with multiple sliding surfaces," *Geotechnical & Geological Engineering*, vol. 14, no. 1, pp. 51–66, 1996.

[36] Q. H. Zhang, "Advances in three-dimensional block cutting analysis and its applications," *Computers and Geotechnics*, vol. 63, pp. 26–32, 2015.

[37] J. R. Moore, M. S. Thorne, K. D. Koper et al., "Anthropogenic sources stimulate resonance of a natural rock bridge," *Geophysical Research Letters*, vol. 43, no. 18, pp. 9669–9676, 2016.

[38] R. Jimenez-Rodriguez and N. Sitar, "Influence of stochastic discontinuity network parameters on the formation of removable blocks in rock slopes," *Rock Mechanics and Rock Engineering*, vol. 41, no. 4, pp. 563–585, 2008.

[39] B. H. Kim, M. Cai, P. K. Kaiser, and H. S. Yang, "Estimation of block sizes for rock masses with non-persistent joints," *Rock Mechanics and Rock Engineering*, vol. 40, no. 2, pp. 169–192, 2007.

[40] T. Backers, O. Stephansson, and E. Rybacki, "Rock fracture toughness testing in Mode II—punch-through shear test," *International Journal of Rock Mechanics and Mining Sciences*, vol. 39, no. 6, pp. 755–769, 2002.

[41] T. Backers, G. Dresen, E. Rybacki, and O. Stephansson, "New data on Mode II fracture toughness of rock from the punch-through shear test," *International Journal of Rock Mechanics and Mining Sciences*, vol. 41, no. 3, pp. 351-352, 2004.

[42] S. Huang, X. T. Feng, and K. Xia, "A dynamic punch method to quantify the dynamic shear strength of brittle solids," *Review of Scientific Instruments*, vol. 82, no. 5, article 053901, 2011.

[43] D. Liu, L. Shen, F. Guillard, and I. Einav, "Transition failure stress in a chain of brittle elastic beads under impact," *International Journal of Impact Engineering*, vol. 93, pp. 222–230, 2016.

[44] J. Zhu, S. Hu, and L. Wang, "An analysis of stress uniformity for concrete-like specimens during SHPB tests," *International Journal of Impact Engineering*, vol. 36, no. 1, pp. 61–72, 2009.

[45] I. Maekawa, "The influence of stress wave on the impact fracture strength of cracked member," *International Journal of Impact Engineering*, vol. 32, no. 1-4, pp. 351–357, 2005.

[46] Q. B. Zhang and J. Zhao, "A review of dynamic experimental techniques and mechanical behaviour of rock materials," *Rock Mechanics and Rock Engineering*, vol. 47, no. 4, pp. 1411–1478, 2014.

[47] K. Xia and W. Yao, "Dynamic rock tests using split Hopkinson (Kolsky) bar system – a review," *Journal of Rock Mechanics and Geotechnical Engineering*, vol. 7, no. 1, pp. 27–59, 2015.

[48] S. Wang, P. Ni, and M. Guo, "Spatial characterization of joint planes and stability analysis of tunnel blocks," *Tunnelling and Underground Space Technology*, vol. 38, pp. 357–367, 2013.

[49] S. Wang and P. Ni, "Application of block theory modeling on spatial block topological identification to rock slope stability analysis," *International Journal of Computational Methods*, vol. 11, no. 1, article 1350044, 2014.